

Channel Based Design of Systems with Multiple Antennas

Tobias Mahler^{1, *}, Lars Reichardt², Christoph Heine¹, Mario Pauli¹, and Thomas Zwick¹

Abstract—In this article a method of optimizing wireless communication systems using multiple antennas is presented. This method focuses on the synthesis of antenna radiation patterns that are optimized in terms of mutual information, taking into account the specific limitations of the antenna design, such as the available space (for the antenna structure), polarization, number and arrangement of the antennas.

1. INTRODUCTION

Multiple-input-multiple-output (MIMO) antenna systems have the potential to increase the mutual information of wireless communication, through additional antennas, hence more channels and hardware. In contrast to the antennas, which are usually quite inexpensive, the size, complexity and price of the front-ends scale with the number of antennas. Accordingly, it is of interest for commercial applications, to use as few system inputs and outputs as possible to reduce the hardware for cost saving.

The performance of a MIMO-antenna system is a direct result of the channel transfer matrix \mathbf{H} , which in turn depends on the propagation environment and the antennas. Since the environment usually cannot be changed, the choice of antennas is crucial for the overall system behavior. The antennas determine inherently the correlation between the transmission coefficients of the channel matrix and, consequently, the mutual information of the system. The number of degrees of freedom (NDF) in the antenna design are: the spatial separation of the antennas, their polarization and their respective complex directional characteristics.

The interaction of the propagation environment with the antennas and the high NDFs make the development of such a system especially time-consuming and expensive. This is the reason why, in most cases, a heuristic approach is used. This means that a certain antenna configuration is chosen based on general assumptions about the propagation environment, knowing that by doing so it is not guaranteed whether this choice increases the potential mutual information or not. Afterwards a prototype set-up with several possible combinations and a subsequent verification by measurements is omitted typically due to cost and time constraints. In contrast to the heuristic approach, our proposal includes full consideration of the propagation environment. The simulations performed during the proposed antenna synthesis method are reproducible and we can expect a resulting antenna system that is optimized in terms of mutual information in time variant mobile channels. Our promise is that this will allow the use of MIMO systems in industrial applications which are (typically) not realizable due to cost and space reasons and due to the high complexity.

The basic idea behind the synthesis presented in this article is to optimize antenna systems by using channel knowledge already in the design process of the system. This enables us to determine fixed directional patterns that are optimized in terms of mutual information for any given set of constraints such as the number of antennas, their geometrical sizes and/or their polarization. By doing so hardware costs can be reduced since a system with fewer but more optimized antennas may have the same performance as a heuristically designed system with multiple antennas.

Received 8 September 2015, Accepted 9 November 2015, Scheduled 10 November 2015

* Corresponding author: Tobias Mahler (tobias.mahler@kit.edu).

¹ Institut für Hochfrequenztechnik und Elektronik (IHE), Karlsruhe Institute of Technology (KIT), Karlsruhe 76131, Germany. ² AUDI AG, Ingolstadt 85045, Germany.

Previous publications that deal with these problems and with alternative radiation pattern synthesis approaches lack the consideration of realistic mobile communication scenarios or focus only on a few distinct channel realizations [1–3]. They do not take into account the fact that mobile channels may vary considerably over time or over changing transmitter or receiver positions whereas our approach aims at optimizing radiation patterns for an average propagation behaviour of variant mobile channels. There are publications that deal with capacity maximizing geometrical array configurations using channel models that incorporate spatial correlation and mutual coupling, e.g., [4, 5]. However our work gives an approach of a radiation pattern synthesis for realistic variant mobile channels. The sampling arrays are only utilized to obtain volume based channel knowledge for the synthesis procedure.

The general idea behind this antenna synthesis has been published in [6–9], furthermore a few application examples for using this methodology for the design of automotive antennas and indoor communication systems are available in [10–12]. This article describes for the first time in depth the fundamentals, the math and the approaches to adapt the synthesis to different NDFs and different design objectives. Furthermore an approach is presented showing how this methodology can be applied on measured channel data.

Section 2 describes the antenna synthesis procedure in detail for invariant channels. Afterwards Section 3 extends the synthesis to time variant channels with the application of averaging strategies. Section 4 generalizes the radiation pattern synthesis procedure for additional degrees of freedom. Section 5 describes the evaluation criteria in brief and Section 6 gives synthesis examples for measured invariant channels. Section 7 then applies the synthesis to simulated variant channels and demonstrates the results. Section 8 then concludes the work.

2. SYNTHESIS APPROACH

The term antenna synthesis describes the procedure of finding optimized antenna characteristics (e.g., the radiation pattern) by evaluating the available knowledge about the channel that the antenna is supposed to operate in.

First the channel knowledge is acquired by channel simulations of realistic scenarios. Hence the channel needs to be sampled. From the channel sampling results we find optimal available subchannels and thus orthogonal radiation patterns for each snapshot (moment in time) of the channel can be determined as typically done in multiplexing systems [13, 14]. Afterwards the antenna synthesis determines radiation patterns and subchannels in dependence of predetermined design constraints. These radiation patterns take advantage of multipaths by using multiple parallel data links (subchannels) at the same time without interference.

2.1. Intrinsic Capacity and the Concept of Antenna Sampling

The achievable capacity (as the maximum of the mutual information) is limited by the receiver and transmitter volume. This is partly due to the fact that the volume defines the aperture of the antenna. The aperture again defines the main beam width and with that the gain or directivity of the antenna. Both limit the number and also the strength of the subchannels that can be used. The capacity is fixed if the complete channel information of the available volume is known.

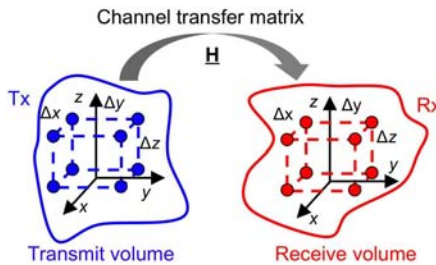


Figure 1. Concept of sampling antennas [6].

In [9, 15, 16], this is shown and designated as intrinsic or spatial capacity. The capacity value can be determined by sampling the transmitting and receiving volume with ideal (sampling) antennas. Fig. 1 illustrates this approach. The sampling antennas are ideal field probes and have no physical size and no mutual coupling. The capacity value saturates when a certain number of sampling antennas is reached in the given volumes. Fig. 2 shows this for a linear array of the length L consisting of equidistantly arranged isotropic radiators for a snapshot (one moment in time) of a simulated urban outdoor channel.

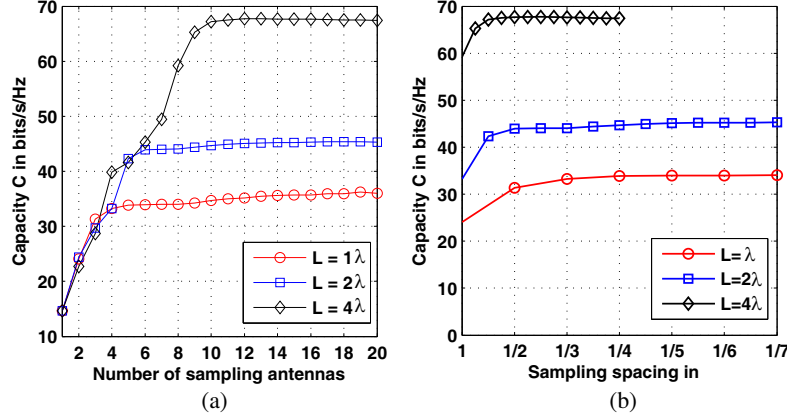


Figure 2. Determined intrinsic capacity for linear antenna arrays of the length L for a snapshot of an urban outdoor channel, (a) against the number of sampling antennas, (b) against the sampling spacing.

The capacity converges to a maximum value for each array size with higher sampling resolutions. This is due to the fact that on the one hand no additional information can be obtained from the $\underline{\mathbf{H}}$ -matrix and that on the other hand the antenna gain for a fixed aperture and therefore also the signal-to-noise-ratio (SNR) saturates. Because of the limited main beam width no additional orthogonal radiation patterns can be determined. Therefore an optimal number of sampling-elements for a given aperture exists that achieves the maximum intrinsic capacity. Exceeding this number results in no additional capacity gain. This fact has also been observed in the theoretical work in [2]. The Nyquist-Shannon sampling theorem, which says that a band-limited signal can be reproduced exactly if the sampling rate is at least twice the maximum occurring signal frequency also applies to the sampling of the radio channel with a large angle-spreading [16]. For such a radio channel with a large angular spread (e.g., evenly distributed scatterers in the vicinity), the optimal number of sampling antennas M_{opt} at the transmitter and N_{opt} at the receiver along the cartesian dimensions x, y, z are given by [16]:

$$N_{x,\text{opt}} = M_{x,\text{opt}} = \frac{2L_x}{\lambda} + 1 \quad (1)$$

$$N_{y,\text{opt}} = M_{y,\text{opt}} = \frac{2L_y}{\lambda} + 1 \quad (2)$$

$$N_{z,\text{opt}} = M_{z,\text{opt}} = \frac{2L_z}{\lambda} + 1 \quad (3)$$

with

$$M_{\text{opt}} = N_{\text{opt}} = M_{x,\text{opt}} \cdot M_{y,\text{opt}} \cdot M_{z,\text{opt}} = N_{x,\text{opt}} \cdot N_{y,\text{opt}} \cdot N_{z,\text{opt}} \quad (4)$$

$$M = N = M_x \cdot M_y \cdot M_z = N_x \cdot N_y \cdot N_z \quad (5)$$

which corresponds to a $\lambda/2$ -sampling, with λ being the wave length and M and N being the total number of sampling antennas at the transmitter and the receiver respectively. Here, it is assumed that the same number of transmitting and receiving antennas is used. If the angular spread of the channel is small, also a smaller number of ideal antennas is sufficient for sampling the $\underline{\mathbf{H}}$ -matrix, since the spatial self-similarity (spatial correlation) of the radio channel is higher.

Based on the intrinsic capacity a reduced number of sampling antennas ($N < N_{\text{opt}}$ and accordingly $M < M_{\text{opt}}$) gives a lower capacity. However small apertures with only a few sampling points may

benefit from a slight over-sampling. The results in Fig. 2(b) confirm this as the saturation begins at sampling spacings smaller than $\lambda/2$ for smaller apertures. $N_{x,\text{opt}} = 3, 5, 9$ represent the number of optimal sampling elements for the linear array lengths of $L_x = 1\lambda, 2\lambda, 4\lambda$.

For a two (2D) and three dimensional (3D) aperture (a surface or a cube), this is shown in Fig. 3(a) and Fig. 3(b). Due to the high number of sampling points, the intrinsic capacity is almost reached for sampling intervals of $\lambda/2$. Again isotropic radiators are assumed to ensure an optimal spatial sampling.

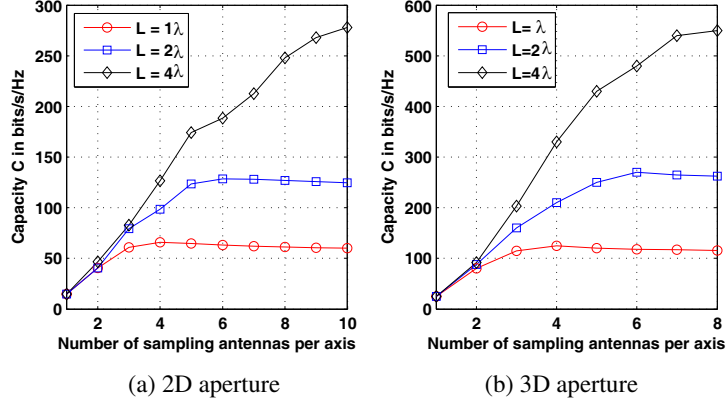


Figure 3. Determined intrinsic capacity for a 2D (a) and 3D (b) array.

2.2. Beam-Forming through Channel Diagonalization

The sampled channel transfer matrix \mathbf{H} contains information about the paths in a multipath propagation environment. In order to transmit data over orthogonal subchannels, or to obtain de-correlated signals, \mathbf{H} must be transformed into a diagonal matrix. This is achieved with aid of the singular value decomposition (SVD):

$$\mathbf{H} = \mathbf{U}\mathbf{S}\mathbf{V}^\dagger, \quad (6)$$

$$\mathbf{S} = \mathbf{U}^\dagger\mathbf{H}\mathbf{V}, \quad (7)$$

where \mathbf{S} is a diagonal matrix and $(\cdot)^\dagger$ denotes the complex conjugate transpose. The diagonal elements of \mathbf{S} consist of the singular values, the non-negative square roots of the eigenvalues λ_i of $\mathbf{H}\mathbf{H}^\dagger$ respectively. The matrices \mathbf{U} and \mathbf{V}^\dagger are unitary beam-forming matrices. Fig. 4 illustrates the principle of the channel diagonalization. By applying the SVD algorithm the excitation vectors are given by the column vectors \vec{v}_i of \mathbf{V}

$$\mathbf{V} = \begin{pmatrix} \vec{v}_1 & \vec{v}_2 & \cdots & \vec{v}_M \\ \underline{v}_{11} & \underline{v}_{12} & \cdots & \underline{v}_{1M} \\ \underline{v}_{21} & \underline{v}_{22} & \cdots & \underline{v}_{2M} \\ \vdots & \vdots & \ddots & \vdots \\ \underline{v}_{M1} & \underline{v}_{M2} & \cdots & \underline{v}_{MM} \end{pmatrix} \quad (8)$$

and \vec{u}_i^* of \mathbf{U}^* respectively. $(\cdot)^*$ denotes the complex conjugate. These vectors determine the signal distribution for each antenna element in order to transmit over orthogonal subchannels. The radiation patterns belonging to these subchannels can be determined using the resultant electric fields [8]. The electric field of the transmitter is given by

$$\vec{E}_i^{\text{Tx}}(d, \theta, \psi) = \frac{e^{-j\beta d}}{d} \sum_{m=1}^M \underline{v}_{mi} \hat{\vec{E}}_m(d, \theta, \psi) e^{j\beta \Delta \varphi_m} \quad (9)$$

and similarly for the receiver by

$$\vec{E}_i^{\text{Rx}}(d, \theta, \psi) = \frac{e^{-j\beta d}}{d} \sum_{n=1}^N \underline{u}_{ni}^* \hat{\vec{E}}_n(d, \theta, \psi) e^{j\beta \Delta \varphi_n}. \quad (10)$$

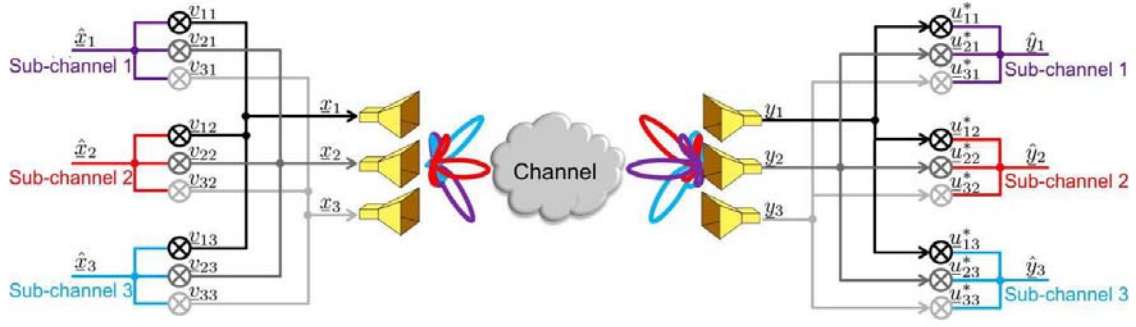


Figure 4. Block diagram of a MIMO-system with pre- and post-processing.

with $\hat{\underline{E}}_m(d, \theta, \psi)$ and $\hat{\underline{E}}_n(d, \theta, \psi)$ denoting the electric field (in far field) of the m -th transmit and n -th receive sampling antenna. θ and ψ represent the elevation and azimuth angles of the spherical coordinate system and d is the distance. The elements of the column vectors of $\underline{\mathbf{V}}$, and of the row vectors of $\underline{\mathbf{U}}^\dagger$ correspond to the excitation coefficients of the antenna elements (m, n) of the i -th subchannel. The phase term $\Delta\varphi$ depends on the relative spatial separation $(\Delta x, \Delta y, \Delta z)$ of the sampling antennas:

$$\Delta\varphi = \Delta x \cdot \sin(\theta) \cdot \cos(\psi) + \Delta y \cdot \sin(\theta) \cdot \sin(\psi) + \Delta z \cdot \cos(\theta) \quad (11)$$

The propagation constant is denoted by β . The radiation patterns for the transmitting and the receiving case can be calculated by

$$\vec{\underline{C}}_i^{Tx}(\theta, \psi) = c_{\text{norm}_i}^{Tx} \sum_{m=1}^M \underline{v}_{mi} \hat{\underline{C}}_m^{\text{samp}}(\theta, \psi) e^{j\beta\Delta\varphi_m} \quad (12)$$

$$\vec{\underline{C}}_i^{Rx}(\theta, \psi) = c_{\text{norm}_i}^{Rx} \sum_{n=1}^N \underline{u}_{ni}^* \hat{\underline{C}}_n^{\text{samp}}(\theta, \psi) e^{j\beta\Delta\varphi_n} \quad (13)$$

$\hat{\underline{C}}_{m/n}^{\text{samp}}$ refers to the pattern of the m -th or n -th sampling antenna. The constant $c_{\text{norm}_i}^{\text{Tx/Rx}}$ normalizes the resulting patterns to values between 0 and 1. Their directivity D can then be determined by:

$$D = \frac{4\pi}{\int_{\psi=0}^{2\pi} \int_{\theta=0}^{\pi} \left| \vec{\underline{C}}_i^{Rx/Tx}(\theta, \psi) \right|^2 \sin\theta \, d\theta \, d\psi} \quad (14)$$

2.3. Synthesis Procedure in Invariant Channels

In order to synthesize radiation patterns that are optimized in terms of mutual information for a predetermined aperture and number of transmit and receive antennas ($N \times M$ MIMO) the concepts of antenna sampling and beam-forming through channel diagonalization are combined. In this manner, considering isotropic radiators as sampling elements, the SVD of $\underline{\mathbf{H}}$ leads to certain beam-forming vectors for each subchannel. These beam-forming vectors yield ideal radiation patterns for maximizing the mutual information. Here, the subchannel coefficients $\sqrt{\lambda_i}$ are ordered according to their strength, wherein the first subchannel is allocated to the largest (strongest) coefficient $\sqrt{\lambda_1}$. This means that the first subchannel has the largest SNR. An example of this is shown in Fig. 5(a). The graph shows the normalized eigenvalues λ_i for linear antenna arrays of length L when sampling with 10 ideal antennas. The number and strength of the subchannels is dependent on the aperture and the angular spread in the channel. Further discussion on the information content and their dependencies in wireless channels can be found in [9] and [16]. One approach to maximize channel capacity, that is often chosen in literature, is to use as many omnidirectional (or even isotropic) antennas as possible including the same amount of front-ends. Hereby the best directional characteristics for each channel snapshot (moment in time) is

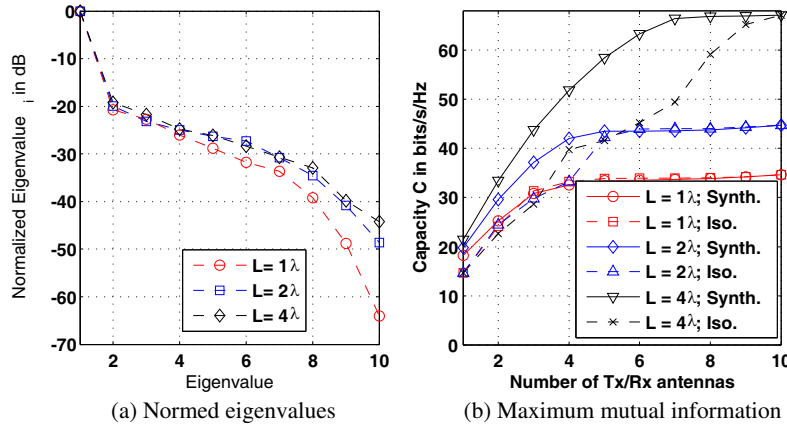


Figure 5. Comparison of the normalized eigenvalues of different linear antenna arrays of length L (a) and the achievable capacity when using isotropic (Iso.) or directive (Synth.) antennas (b).

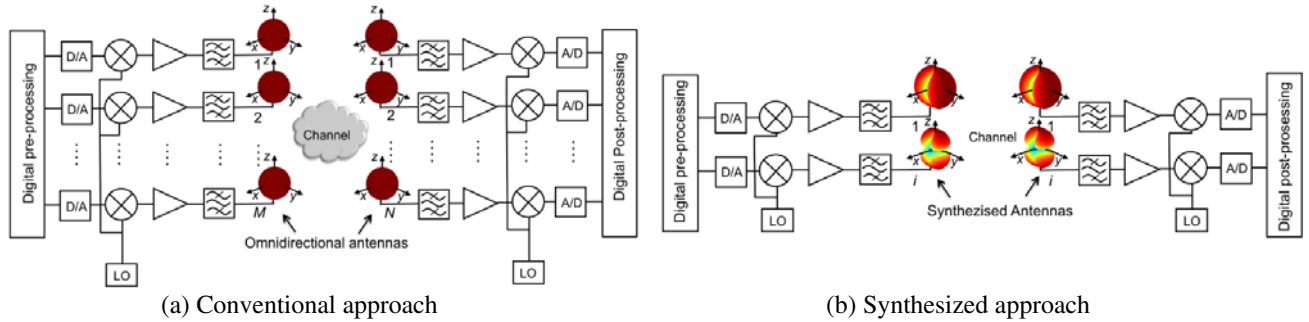


Figure 6. Block diagram of a conventional approach for a system with multiple antennas and of the synthesis approach.

determined by data pre- and post-processing [17]. An obvious disadvantage of such an approach is the very high hardware effort. A less obvious one is the fact that in real channels often only a small number of subchannels with significant power that can be used effectively for communication exist. The idea behind the antenna synthesis is thus, to design systems with multiple antennas with fixed (synthesized) directional patterns. In Fig. 6 this is illustrated by a block diagram. The patterns are focusing on the most powerful subchannels and thus achieve a high mutual information with only a small number of system inputs and outputs. The effect on the mutual information is illustrated by an example in Fig. 5(b). The channel is sampled by linear arrays (of length L) consisting of isotropic antennas. It shows the maximized mutual information as a function of the number of transmit/receive antennas ($N \times M$ MIMO with $N = M$) together with the impact of the synthesized patterns. The synthesis itself is based on channel sampling with 10 elements. The capacities of the directive, synthesized antennas saturate significantly earlier than the one of isotropic antennas. Before the saturation values are reached, the achievable capacity is considerably higher compared to an array of isotropic antennas. This means that for a channel snapshot an optimal solution in terms of patterns for a given aperture and number of system inputs and outputs can be found. The block diagram in Fig. 7(a) of the synthesis for an invariant channel. In the first step, the size and geometry of the aperture, the relevant propagation environment as well as the number of antennas to be designed is determined. By sampling the aperture in the propagation environment the channel matrix \mathbf{H} is determined. The spacing between the sampling antennas should not exceed $\lambda/2$ in order to follow the sampling theorem and to prevent the generation of grating lobes. Using the SVD the excitation coefficients for the sampling antennas are determined for the strongest subchannels. The results of this synthesis are channel orthogonalizing directional radiation patterns for the transmitter and receiver.

3. EXTENSION OF THE SYNTHESIS PROCEDURE FOR TIME VARIANT CHANNELS

The approach to determine an optimal pattern presented in Section 2 only refers to a single snapshot of the channel. In general, the multipath propagation and thus the transmission channel \mathbf{H} is time, location and scenario dependent. Fig. 8 illustrates this using two synthesized directional characteristics at time t_1 and t_2 . Since there is an optimal solution for each snapshot of the channel an averaging approach for the design of fixed radiation patterns becomes necessary. This averaging does not always lead to completely orthogonal channels.

The block diagram in Fig. 7(b) illustrates the data flow for the variant approach. Input parameters are the specifications of the antenna system to be designed (including size of aperture, polarization, locations and number of inputs and outputs), as well as the scenarios. A volume related channel transfer

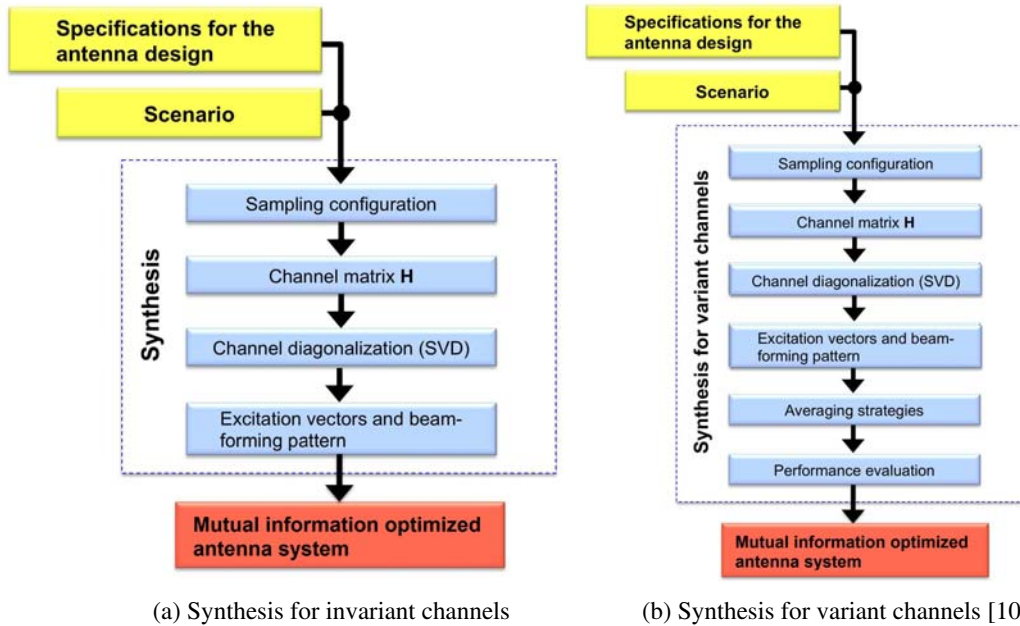


Figure 7. Block diagram of the synthesis processing for invariant (a) and variant (b) channels.

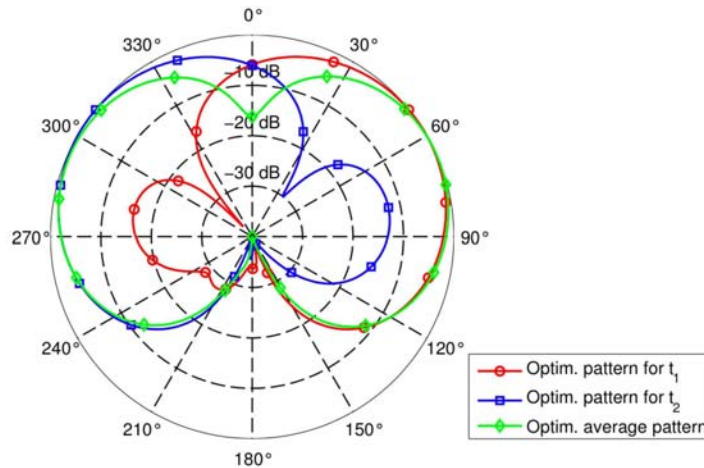


Figure 8. Exemplary determination of an optimum directional pattern for snapshot time t_1 and t_2 , as well as an average solution.

matrix $\underline{\mathbf{H}}$ is determined due to channel simulations and the excitation vectors for each subchannel of each channel snapshot are calculated by the singular value decomposition. Afterwards channel orthogonalizing patterns are determined with the aid of an averaging approach. Specific properties of the overall system can be influenced by the type of averaging strategy chosen. The mutual information can be calculated through a further simulation of the synthesized system. The comparison of the CDFs allow for a consideration and an evaluation of different systems in the same scenarios.

In this subsection, the averaging of the subchannel patterns is described as well as some weighting factors. These weighting factors are used to evaluate the instantaneous solutions and to control their impact on the final synthesized radiation patterns.

3.1. Averaging Approach

The synthesized patterns for each subchannel i are defined by the arrangement of sampling antennas, and by the column vectors \vec{v}_i of the matrix $\underline{\mathbf{V}}$ on transmitter side and the column vectors \vec{u}_i^* of $\underline{\mathbf{U}}^*$ on receiver side. For each channel realization n_{cr} there are optimal excitation vectors $\vec{v}_i(n_{cr})$ and $\vec{u}_i^*(n_{cr})$, for each i -th subchannel. Depending on the number of antennas N_s to be synthesized only the first vectors $i = 1 \dots N_s$, are taken into account. The result of the averaging provides the excitation vectors $\bar{\vec{v}}_i$ and $\bar{\vec{u}}_i^*$ ($i = 1 \dots N_s$).

In the following the averaging is described with the transmitter excitation vectors, but can identically be applied to the receiver vectors. If receiver and transmitter use the same radiation pattern, the averaging can be applied with \vec{v}_i and \vec{u}_i^* together. The averaged synthesized patterns $\bar{\underline{\mathbf{C}}}_i^{\text{synth}}(\theta, \psi)$ can then be determined by (12) and rewritten as

$$\bar{\underline{\mathbf{C}}}_i^{\text{synth}}(\theta, \psi) = c_{\text{norm}i} \sum_{m=1}^M \bar{v}_i \hat{\underline{\mathbf{C}}}_m^{\text{samp}}(\theta, \psi) e^{j\beta\Delta\varphi_m^{\text{samp}}}. \quad (15)$$

Here, \bar{v}_{mi} denotes the average coefficients for each excitation and $\hat{\underline{\mathbf{C}}}_m^{\text{samp}}(\theta, \psi)$ the pattern of the sampling antennas. The easiest way to get an averaged solution is the use of simple mean (SM) by

$$\bar{\vec{v}}_i = \frac{\sum_{n_{cr}=1}^{N_{cr}} \vec{v}_i(n_{cr})}{N_{cr}}, \quad (16)$$

where N_{cr} is the total number of considered snapshots. With the approach in (16) all instantaneous solutions are weighted equally. Alternatively, an average of

$$\bar{\vec{v}}_i = \frac{\sum_{n_{cr}=1}^{N_{cr}} w(n_{cr}) \vec{v}_i(n_{cr})}{\sum_{n_{cr}=1}^{N_{cr}} w(n_{cr})} \quad (17)$$

can be applied. With $w(n_{cr})$ being the weight of the n_{cr} -th channel realization. In the case of weighted averaging the solutions of certain snapshots are preferred. Possible weighting functions are:

- The Frobenius norm $\|\cdot\|_F$ of $\underline{\mathbf{H}}$

$$w(n_{cr}) = \|\underline{\mathbf{H}}(n_{cr})\|_F = \sqrt{\sum_{n=1}^N \sum_{m=1}^M |\underline{h}_{n,m}(n_{cr})|^2}. \quad (18)$$

It gives a good approximation for the mean attenuation of the MIMO communication channel at the time n_{cr} . Therefore snapshots with a strong line-of-sight component are preferred.

- The power of the individual transmission coefficients ($h_{1,1}$)

$$w(n_{cr}) = |\underline{h}_{1,1}(n_{cr})|^2. \quad (19)$$

Similar to the weight of the Frobenius norm strong subchannels are weighted higher. However here only the first subchannel is considered.

- The Eigenvalue dispersion (EVD) [9]

$$w(n_{cr}) = \frac{\left(\prod_{i=1}^{N_s} \lambda_i(n_{cr}) \right)^{\frac{1}{N_s}}}{\frac{1}{N_s} \sum_{i=1}^{N_s} \lambda_i(n_{cr})}. \quad (20)$$

The EVD describes the relationship between geometric and arithmetic mean of the eigenvalues λ_i with $i = 1 \dots N_s$ [18]. Evaluated are the relative power differences of the resulting subchannels and thus their distribution. The EVD takes values between zero and one. A value of one means that all considered subchannels have the same power which favors multiplexing and leads to a high capacity.

3.2. Pattern Allocation

When $N_s \geq 2$, each snapshot yields channel orthogonalizing radiation patterns. By the averaging approach, as has been described by (16) and (17), the orthogonalizing property will almost always be lost. However, as it will be shown later, the averaging approach still results in a better performance than systems that are designed without the antenna synthesis method. In addition, it may happen that, although the excitation vectors $\underline{\vec{v}}_1(n_1)$ and $\underline{\vec{v}}_2(n_1)$, and thus the patterns for the first snapshot are orthogonal, in the following snapshot the second subchannel pattern $\underline{\vec{v}}_2(n_2)$ focuses towards the same direction as the first subchannel pattern in the first snapshot. In this case it would be better to average $\underline{\vec{v}}_1(n_1)$ with $\underline{\vec{v}}_2(n_2)$, and $\underline{\vec{v}}_2(n_1)$ with $\underline{\vec{v}}_1(n_2)$.

To account for this, for example by a $N_s = 2$ synthesis, the first and second subchannel averaging is no longer fixed. It is rather an association with regard to the similarity of the excitation vectors. Mathematically, the similarity of two vectors is evaluated by the standard dot product. The value of the standard dot product rises with increasing similarity of the two vectors. Equation (17) can now be extended to include this correlation. The averaging is done by consecutive channel realizations

$$\bar{\underline{\vec{v}}}_i = \frac{\sum_{n_{cr}=1}^{N_{cr}} w(n_{cr}) \underline{\vec{v}}_{sub_i(n_{cr})}(n_{cr})}{\sum_{n_{cr}=1}^{N_{cr}} w(n_{cr})}. \quad (21)$$

For the simple mean, $w(n_{cr})$ equals 1. The subscripted $sub_i(n_{cr})$ indicates the subchannel of the n_{cr} -th snapshot and is given for $n_{cr} \neq 1$ by

$$sub_i(n_{cr}) = j : 1 \leq j \leq N_s, \quad |\langle \underline{\vec{v}}_j(n_{cr}), \bar{\underline{\vec{v}}}_i(n_{cr} - 1) \rangle| = \max!. \quad (22)$$

For each snapshot $n_{cr} \geq 2$ the dot product between the current snapshot $\underline{\vec{v}}_j(n_{cr})$ and the current averaged excitation $\bar{\underline{\vec{v}}}_i(n_{cr} - 1)$ is calculated. Furthermore the vector $\underline{\vec{v}}_j(n_{cr})$ is chosen to maximize the dot product to take the subchannel similarities into account.

In the time and environment invariant case, a large aperture leads to very directive directional patterns. The averaging approach for variant channels leads, depending on the channel variance, again to less directive patterns. Therefore, in the case of averaging, patterns may result, which can be realized with a smaller aperture than that used for the sampling. Accordingly an optimum aperture size for the considered scenarios may result.

3.3. Phase Correction

The fact that the excitation vectors are complex has been neglected so far. However, the beam-forming depends only on the relative phase differences between the excitation coefficients, so the same main-beam directions can be created by different excitation vectors. This is considered in (22) by the absolute of the dot product. The phase describes the relative phase difference between the beam-forming patterns and was not considered so far. Since the averaging is coherent, it may lead to anti-phase excitation vectors. To avoid this, a phase adjustment for each newly assigned averaging vector is performed. Equation (22) is thus extended to

$$\vec{v}_i = \frac{\sum_{n_{cr}=1}^{N_{cr}} w(n_{cr}) \vec{v}_{sub_i(n_{cr})}(n_{cr}) e^{j\Delta\Phi_i(n_{cr})}}{\sum_{n_{cr}=1}^{N_{cr}} w(n_{cr})} \quad (23)$$

with the phase correction term $\Delta\Phi_i(n_{cr})$, determined for $n_{cr} \neq 1$ by

$$\Delta\Phi_i(n_{cr}) = \arg \left\{ \langle \vec{v}_{sub_i(n_{cr})}(n_{cr}), \vec{v}_i(n_{cr} - 1) \rangle \right\}. \quad (24)$$

3.4. Threshold Decisions of the Number of Relevant Subchannels

So far, the number of observed subchannels for the synthesis equals the number of radiation patterns. An alternative option is to consider either an absolute T_{abs} or a relative threshold level T_{rel} for the power of the subchannels.

T_{rel} refers to the difference to the strongest (first) subchannel, T_{abs} to the eigenvalues of λ_i . By the use of a threshold the number of considered excitation vectors becomes variable. This may have the advantage that weak subchannels of some snapshots are not included in the averaging, or that in channels where the number of relevant subchannels is larger more excitation vectors are considered and the fitting ones can be chosen for the averaging.

4. TAKING INTO ACCOUNT DIFFERENT DEGREES OF FREEDOM FOR THE MULTI-ANTENNA SYNTHESIS

Traditionally for *diversity*, multiple copies of information are sent and/or received to increase the SNR at the receiver [19]. De-correlated receive signals are thus necessary for a high *diversity* gain. Multiple orthogonal subchannels can be used only if it is possible to diagonalize the transfer matrix. In this case different data streams are transmitted via these subchannels (*multiplexing*) and the throughput and the spectral efficiency can be maximized. This proposed synthesis, based on the SVD, is able to support both the principles of *diversity* and *multiplexing* by synthesizing patterns that generate strong, de-correlated subchannels.

Up to now only the radiation patterns are used as the degree of freedom. The number of design degrees can be further increased by considering the polarization and/or the arrangement of the antennas in space. The number of the degrees of freedom used depends on the constraints of the antenna system to be designed. This section discusses the different degrees of freedom and their involvement in the synthesis.

4.1. Degree of Freedom: Pattern

For the cases in which the antennas in a MIMO system have different patterns, as shown in Fig. 9, the system benefits from *pattern diversity*. This can be realized for example by means of a multi-mode antenna. High capacity can be achieved in this case if the patterns are able to orthogonalize the transmission channel. So far, the presented synthesis has focused on this type of *diversity*. This can be determined by the excitation coefficients resulting from the SVD of $\underline{\mathbf{H}}$ for the scanning antennas used. If it is a time and/or site-variant antenna system, only an averaged solution can be determined (see

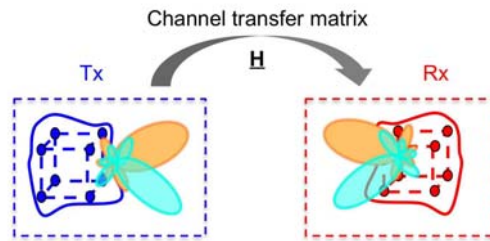


Figure 9. Principle of *pattern diversity*.

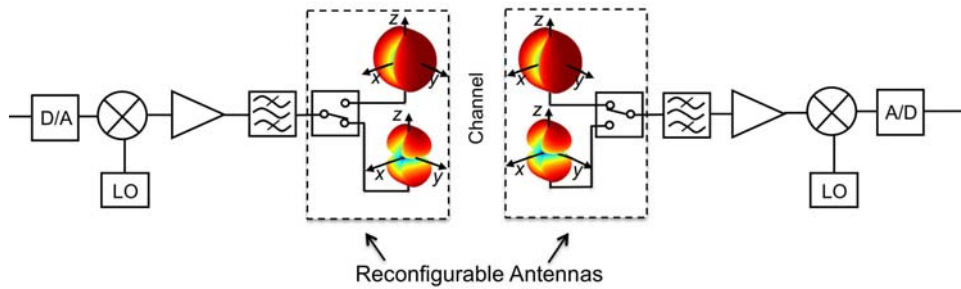


Figure 10. Block diagram of a synthesized antenna system with reconfigurable antennas.

Section 3). The results of this averaging are therefore channel orthogonalizing patterns. An alternative to a system composed of several synthesized directional patterns, which are operated in parallel as shown in the block diagram in Fig. 6(b) arises by the use of reconfigurable antennas. A block diagram for such an approach is given in Fig. 10. Here reconfigurability with respect to the radiation patterns is assumed. The directional patterns could then represent the results of syntheses in different channels so that the antenna system is able to adapt to the environment.

4.2. Degree of Freedom: Spatial Separation

A widespread and simple solution for the antenna design of a MIMO-system is to take identical antenna elements and to separate them physically. Fig. 11 illustrates the principle of this so-called *space diversity* systems. The mutual information gain is not received by channel orthogonalizing patterns, but by the spatial separation of the antennas and the space selective behavior of the channel. Furthermore, for the case where multiple volumes are available for the antenna design, a multi-location synthesis can be used to determine the mutual information maximizing patterns. In the following, it is assumed that the systems at each, the transmitter and receiver side, consist of two separated antenna locations (*A* and *B*

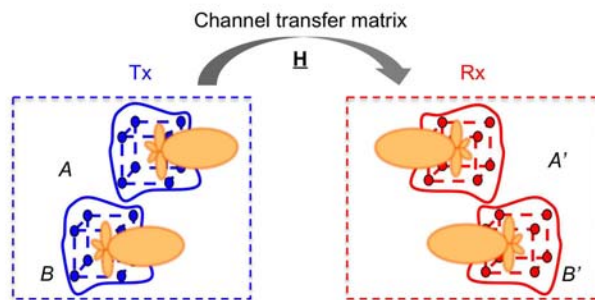


Figure 11. Principle of *space diversity*.

for transmitter and A' and B' for receiver). The following principles can however be extended to any number of antenna sites. For this 2×2 system the associated channel matrix is given by

$$\underline{\mathbf{H}} = \begin{pmatrix} \underline{\mathbf{H}}_{A'm,An} & \underline{\mathbf{H}}_{A'm,Bn} \\ \underline{\mathbf{H}}_{B'm,An} & \underline{\mathbf{H}}_{B'm,Bn} \end{pmatrix}. \quad (25)$$

Since the target of the synthesis is to determine a pattern each for both locations, only the sub-matrices $\underline{\mathbf{H}}_{A'm,An}$ and $\underline{\mathbf{H}}_{B'm,Bn}$ are considered. By use of the SVD together with the use of a threshold decision the excitation coefficients for the strongest subchannels are calculated. The resulting excitation vectors can then be weighted according to Subsection 3 and averaged to achieve a solution for time-variant systems. It should be noted that the averaging over both sites is only useful if both have equal and equally oriented volumes. If this is not the case, the resulting patterns might not be physically realizable for the given apertures.

4.3. Degree of Freedom: Spatial Separation and Pattern

In the previous sub-section the diversity gain is achieved solely by the spatially selective behavior of the channel. In general, better results can be achieved if the patterns are different at spatially separated locations as shown in Fig. 12. Besides the possibility to generate un-correlated channels by the additional degree of freedom, especially the option to use an unequal size and/or kind of volumes offers the possibility to adjust the antennas to the specific multi-location requirements. For the multiple site syntheses different approaches can be pursued:

- The simplest approach is to consider (see Subsection 4.2) only the matrices $\underline{\mathbf{H}}_{A'm,An}$ and $\underline{\mathbf{H}}_{B'm,Bn}$ and to synthesize a radiation pattern for each site separately. This approach can be easily adapted to specific design goals, such as the de-correlation of the channels $A'A$ and $B'B$. By considering several subchannels for each location excitation vectors can be determined that minimize the cross-matrices $\underline{\mathbf{H}}_{A'm,Bn}$ and $\underline{\mathbf{H}}_{B'm,An}$.
- If both antennas transmit the same information the synthesis is carried out with reference to the following matrices

$$\begin{pmatrix} \underline{\mathbf{H}}_{A'm,An} \\ \underline{\mathbf{H}}_{B'm,An} \end{pmatrix}, \quad \begin{pmatrix} \underline{\mathbf{H}}_{A'm,Bn} \\ \underline{\mathbf{H}}_{B'm,Bn} \end{pmatrix}, \quad (26)$$

$$\begin{pmatrix} \underline{\mathbf{H}}_{A'm,An} \\ \underline{\mathbf{H}}_{A'm,Bn} \end{pmatrix}, \quad \begin{pmatrix} \underline{\mathbf{H}}_{B'm,An} \\ \underline{\mathbf{H}}_{B'm,Bn} \end{pmatrix}$$

for the locations of A' (receiver), A (transmitter), B' (receiver) and B (transmitter). With this, a SIMO (single-input-multiple-output) synthesis for each receiver and a MISO (multiple-input-single-output) for each transmitter location is performed. If transmitter and receiver should finally use the same antenna, then an averaging over the transmitter and receiver pattern has to be done.

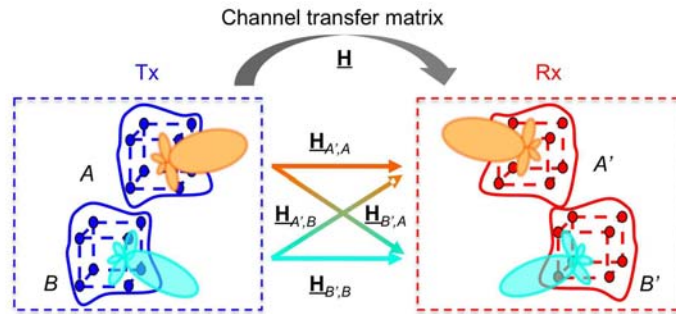


Figure 12. Principle of *space diversity* combined with *pattern diversity*.

- Alternatively, the synthesis can be performed using the entire matrix $\underline{\mathbf{H}}$ of (25). Resulting from the column vectors of the matrices $\underline{\mathbf{V}}$ and $\underline{\mathbf{U}}^*$

$$\underline{\mathbf{V}} = \begin{pmatrix} \vec{v}_1 & \vec{v}_2 & \cdots & \vec{v}_M \\ \underline{v}_{A 11} & \underline{v}_{A 12} & \cdots & \underline{v}_{A 1M} \\ \vdots & \vdots & \ddots & \vdots \\ \underline{v}_{A M1} & \underline{v}_{A M2} & \cdots & \underline{v}_{A MM} \\ \underline{v}_{B 11} & \underline{v}_{B 12} & \cdots & \underline{v}_{B 1M} \\ \vdots & \vdots & \ddots & \vdots \\ \underline{v}_{B M1} & \underline{v}_{B M2} & \cdots & \underline{v}_{B MM} \end{pmatrix} \quad (27)$$

(only $\underline{\mathbf{V}}$ is shown) the coefficients to use can directly be read. The first $A M$ values of the strongest subchannel excitation vector \vec{v}_1 belong to location A , the following $B M$ values to the site B . The orthogonal subchannels arise by the interaction of the patterns of the two sites.

4.4. Degree of Freedom: Polarization and Pattern

If the antennas can make use of different polarizations to create un-correlated channels this is known as *polarization diversity*. This principle is outlined in Fig. 13.

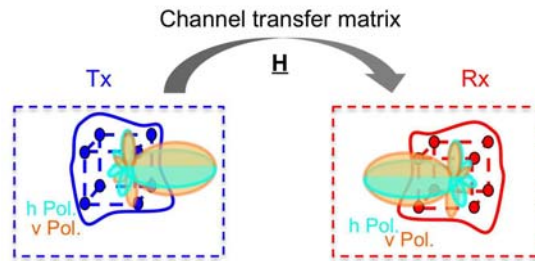


Figure 13. Principle of *polarization diversity* (horizontal h-Pol and vertical v-Pol) combined with *pattern diversity*.

The degree of freedom polarization can be considered by a full polarimetric sampling of the available volume. Similar to (25) the following description of the channel transfer matrix can be used

$$\underline{\mathbf{H}} = \begin{pmatrix} \underline{\mathbf{H}}_{\psi m, \psi n} & \underline{\mathbf{H}}_{\psi m, \theta n} \\ \underline{\mathbf{H}}_{\theta m, \psi n} & \underline{\mathbf{H}}_{\theta m, \theta n} \end{pmatrix}. \quad (28)$$

The subscripts ψ and θ refer to the two orthogonal polarizations at this point. In this type of synthesis, all approaches presented in this subsection can be applied. In addition, a combination of all the degrees of freedom and presented principles can be performed.

5. EVALUATION CRITERIA

The last step for the extended synthesis algorithm is a performance analysis. The synthesized systems are, unless otherwise described, evaluated in terms of mutual information, since this is dependent both on the SNR and on the de-correlation of the subchannels. To maximize them both is an important criteria for the design of multiple-antenna systems to achieve either MIMO or diversity gain. The mutual information is determined by means of simulations considering the synthesized antenna system. Since for each snapshot of a channel, a different mutual information value may result, the cumulative distribution functions (CDF) of the systems are evaluated. Fig. 14 shows such distribution functions. It indicates the undershoot probability of dropping below a certain value. Since for communication purposes often not the maximum achievable mutual information is of interest, but rather the one that is achieved in most cases, the lower part of the CDF curves must be optimized. Based on Fig. 14 this means that the system function 2 is preferable to the system function 1.

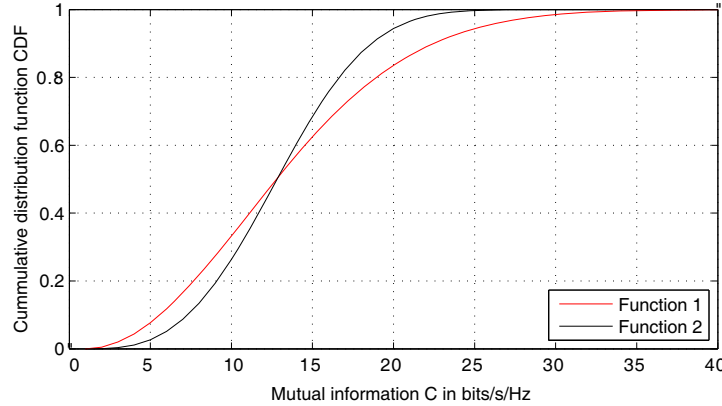


Figure 14. Example of two cumulative distribution functions with different standard deviation.

Alternative Criteria of Optimization

For a given communication standard, it may happen that the standard itself is not properly matched to the channel characteristics. Thus, for example, when the sub-carrier spacing of an OFDM (orthogonal frequency division multiplexing) transmission is chosen to be too low, a high Doppler-spread leads to inter-carrier interference [20]. In this case, directional antennas can be used to effectively reduce the Doppler-spread [21, 22]. With a proper choice of the patterns the angular spectrum is split, so that the same Doppler components fall into one of the subchannel patterns. If a weighting factor is defined for (17) which favors solutions that have a low Doppler-spread, a compromise between maximizing the mutual information and minimizing the Doppler-spread may be found. The same procedure can also be applied for reducing the delay-spread for example, to avoid inter-symbol interference.

6. APPROACH FOR USING MEASURED CHANNELS FOR AN ANTENNA SYNTHESIS

The content of this section is a measurement-based verification of the presented antenna synthesis methodology. In Section 2 it was shown how capacity maximizing directional radiation patterns can be synthesized using spatial sampling and the SVD. The objective now is to design a measurement system, with which the synthesis concept can be verified. The channel sampling takes place in space. To realize this, all transmission coefficients of $\underline{\mathbf{H}}$ are measured serially. This implies that the measurements can be carried out only in time invariant channels, since the channel is not allowed to change during the measuring period. In order to verify the presented methodology, knowledge of the full channel matrix $\underline{\mathbf{H}}$ is necessary. The sampling of the discrete points in space requires a measuring system which can position the sampling antenna along the three axes (x , y and z) in space with sufficient speed and accuracy. Therefore two measuring tables are necessary, one for sampling the transmitting and one for the receiving volume. Fig. 15(a) summarizes the measurement setup schematically, that was used to verify the synthesis. The spatial sampling for the theoretical case assumes ideal field sensors without spatial extension and directional pattern. As this is not possible in the real measurement scenario a compromise must be made, using antennas with omnidirectional patterns e.g., dipoles or monopoles. The use of a real antenna also means that the measurement is not fully polarimetric anymore. If a full-polarimetric $\underline{\mathbf{H}}$ -matrix is desired, then the measurement must be performed separately for both co- and cross-polarizations. For this, two identical $\lambda/4$ -Monopoles designed for operating at 5.9 GHz are used in the following.

The synthesis is based on the idea of the intrinsic capacity which determines the upper bound of the channel capacity regardless of the exact implementation of the antennas, i.e. the capacity that could be achieved by an optimal antenna setup for a specific channel snapshot. In order to determine these directive patterns, the volume must be sampled with ideal field sensors. As a real antenna influences the electromagnetic field due to its size (antenna effective area) and thus changes the intrinsic channel, hence a perfect determination of the intrinsic capacity is therefore not possible. However, an antenna synthesis

based on real measurements allows a comparative evaluation of different antenna configurations that depend on their geometric size.

Another point which has to be taken into account arises from the fact that real antennas are not isotropic and therefore do not cover all directions evenly. The monopoles used as measurement antennas have minima in the $\pm z$ -direction. If this antenna is used for a full-polarimetric measurement and therefore is rotated in the x -direction by 90° the minima rotate so that they are now aligned with the y -axis. This means that by rotating the test antennas (rotation of the polarization) multi paths from certain directions are weighted differently.

In order to verify both the synthesized directions of the main lobes as well as the number of subchannels, different measurement series are carried out in an anechoic chamber. Fig. 15 shows a photograph and a sketch of the antenna measurement chamber. The chamber itself is covered with absorbers to suppress multipath propagation, so that only one relevant propagation path, the Line-of-Sight (LOS) path, exists. By doing so a very controlled environment is provided. A second path is generated deterministically using a reflector. The distance between the two measuring stages is about 5 m. The motor controller, the network analyzer and a personal computer used for controlling the measurement are located outside the chamber, as sketched in Fig. 15(c). Two measurement series are recorded, one with and one without a reflector.

Samples are taken with a resolution of $\lambda/2$ in a $0 \times 2 \times 2 \lambda$ (x, y, z) large area for the transmitter and the receiver. This leads to 25 transmit and 25 receive positions. Scanning a flat surface and the subsequent antenna synthesis based on omnidirectional radiating elements leads to directional patterns, which are mirror-symmetrical to the scanning surface. Fig. 16 illustrates the synthesized directional patterns for the first two subchannels for the case that there is no reflector in the scenario. As expected, the first subchannel uses the LOS path, whereas no preferred direction for the second subchannel can be identified. The resulting directivity for this subchannel, shown in Fig. 16(b), is almost omnidirectional. A reflector is introduced in the scenario for the second measurement series. The reflector is a smooth metal plate, which is aligned with the aid of a laser pointer. The directional characteristics of the first subchannel (Fig. 17(a)) are very similar to those in the case without reflector of the previous scenario (Fig. 16(a)). The slight tilt of the main beam in azimuth is due to the exact alignment of the equipment in the scenario as it is necessary to adjust the additional reflection.

A significant difference becomes visible when the second subchannels, shown in Fig. 16(b) and Fig. 17(b) respectively are considered. For the second setup, the synthesis determines a second directional pattern which focuses towards the reflector. For completeness Fig. 17(c) shows the third subchannel. Since no further strong multipaths exist, the synthesized patterns are quite undirected again. If one considers the directional characteristics in three dimensions, it is noticeable that for

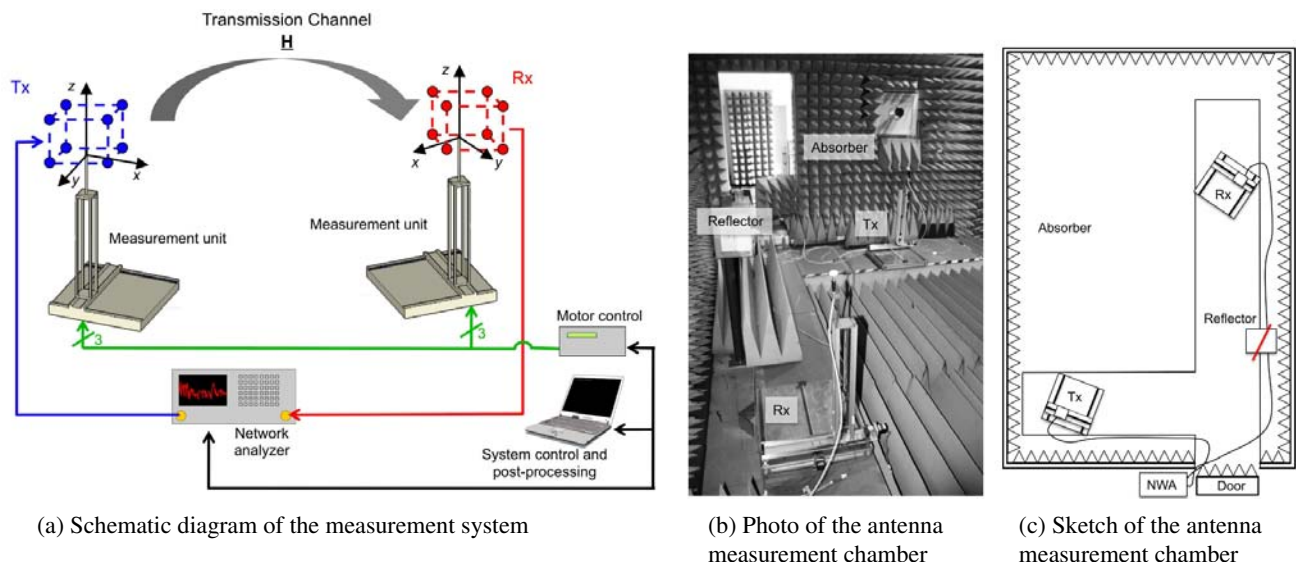


Figure 15. Measurement system applied in the antenna measurement chamber.

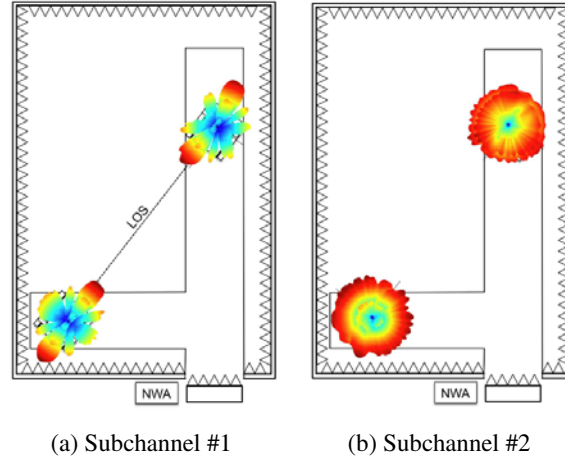


Figure 16. Normalized directional characteristics, no reflector in the scenario.

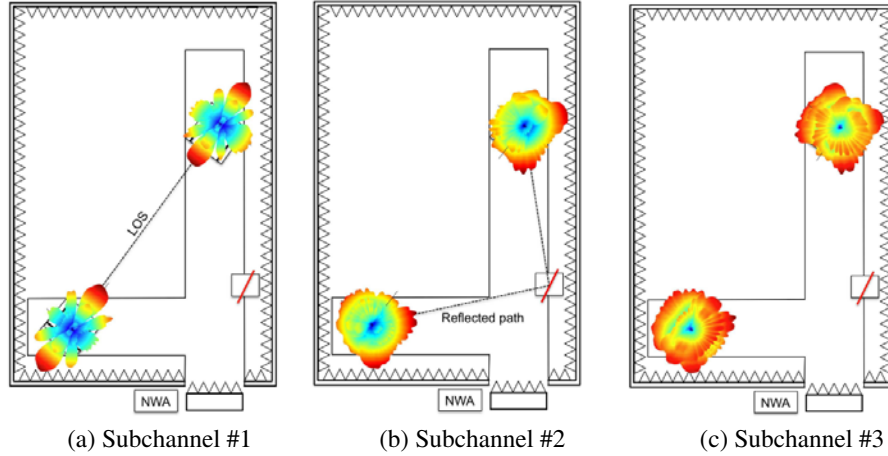


Figure 17. Normalized directional characteristics, reflector in the scenario.

the third subchannel, the directional patterns of the transmitter and receiver possess a minimum in the azimuth plane in order to ensure the orthogonality to the other subchannels. The mutual information for these systems cannot be determined since the channel matrix from the synthesized patterns is needed. However, these measurements fully confirm the synthesis concept and demonstrate the feasibility of spatial sampling with non-ideal antennas.

7. EXAMPLE OF AN ANTENNA SYNTHESIS WITH SIMULATED CHANNELS

The results in this section are taken from [11]. Further information about the sampling details and the antenna volumes leading to these results can be found in the aforementioned publication. They demonstrate the application of the antenna synthesis approach with simulated channels and are therefore included for the sake of completeness. The channel simulations used are performed in typical Car-to-Car (C2C) scenarios and are calculated by a ray-tracing algorithm. Depending on the area in which the traffic setting under investigation is located, different objects occur in the vicinity, including moving cars, parked cars, buildings, road signs and vegetation. For this investigation 16 different antenna locations (shown in the bottom right of Fig. 18) are taken into account. These antenna positions are chosen due to the space availability and the current antenna positions that are typically in use. Based on the particular locations there are limits on the volumes, which have to be sampled for the

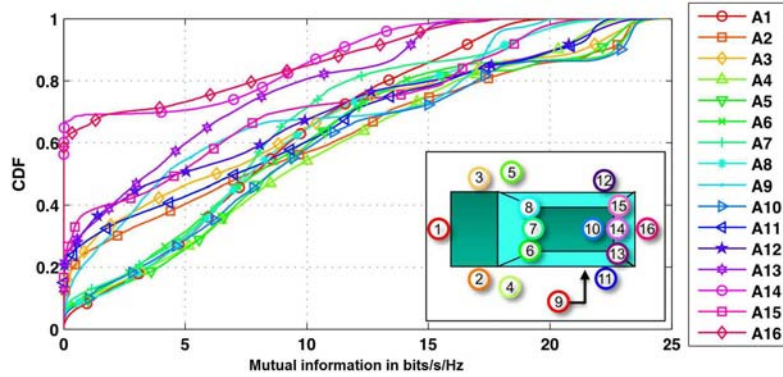


Figure 18. CDFs of all considered antenna locations for the synthesis of a SISO system [11].

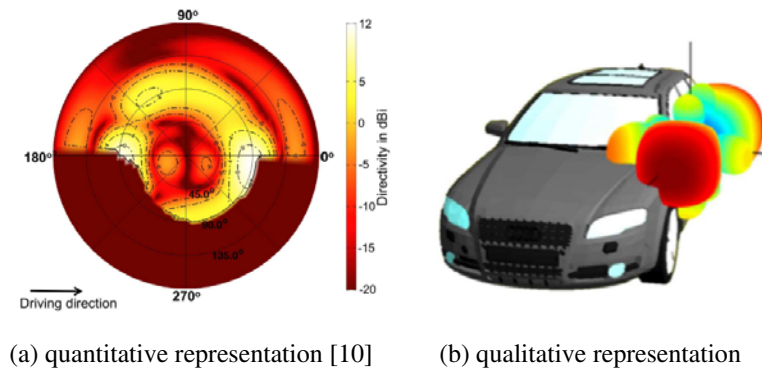


Figure 19. Synthesized radiation patterns for the left side mirror position.

antenna synthesis. To evaluate all antenna positions the cumulative distribution function (CDF) of the transformation is analyzed. For C2C communication it is also not the highest achievable data rate that is important, rather the mutual information achievable for most cases in the lower part of the CDFs. Fig. 18 summarizes the results for synthesizing a SISO system. The best performing antenna positions, taking into account the lower part of the CDFs, have a visibility region that covers \pm the driving direction which are the side mirror positions (A4, A5), the roof antenna position (A10) and the ones at the A-pillar (A6, A8) and in the windshield (A7). Fig. 19 shows the result of the synthesis, the radiation patterns for the positions A4. In Fig. 19(a) the azimuth angle ψ is shown as the tangential component going from 0° to 360° and the elevation angle θ is shown as the radial component of the plot ranging from 0° (zenith) to 90° . It is clear from the figure that all main beam directions focus in \pm driving direction. The main interaction plane is the azimuth one. A study of the angular power spectrums (APS) shows that there is only a small area around ($\theta = 90^\circ$) which is relevant in elevation. Therefore it is of advantage to put the maximum achievable antenna gain in the azimuth plane. The study of the APS in the azimuth plane shows that in C2C communication often a so-called canyon effect is visible. That means that the street is surrounded for instance by buildings, that act like a wave-guide. In case the distance between the receiver and transmitter vehicle is large, then most of the multipath components arrive (or depart) in or against the driving direction. Therefore particularly in non line-of-sight cases the antenna systems benefit if the main beam direction covers these directions. For further information and studies the reader is referred to [10, 11]. The predominant directions of transmission and reception in automotive applications are pointed out very well by the proposed synthesis using the algorithms for variant channels. However since handheld devices may be rotated during operation, the synthesis would come up with no specific directional pattern after the averaging step. This is mainly due to the fact that the wave field around handheld devices shows higher variances in direction and amplitude because of the changes in spatial orientation of the whole device in mobile variant channels.

8. CONCLUSION

The main scientific findings are:

- The capacity of a transmission system, which is in a limited volume, and thus has a finite aperture is limited and saturates in the so-called intrinsic or spatial capacity. For the spatial sampling with ideal field sensors, the intrinsic capacity, is achieved with a sampling spacing of $\lambda/2$, or for a very small volume with a bit less than $\lambda/2$, as shown in Section 2.1.
- With the use of synthesized antennas the number of antenna elements of the system can be reduced, while achieving the same capacity, as shown in Section 2.3.
- An averaging approach allows to extend the synthesis to time, location, and scenario variant channels. Specific properties of the system with multiple antennas can be achieved (for example, a reduction of the Doppler-spread) through various weighting factors applied with the averaging.
- When applying an averaging strategy, directivity might decrease due to a wider main lobe and thus result in an optimal aperture for the given scenarios and applications.
- For the first time, a synthesis is done on basis of a measured channel sampling.

REFERENCES

1. Murata, K. and N. Honma, "Analysis of maximum channel capacity for linear antennas using method of moments," *2011 International Symposium on Antennas and Propagation (ISAP 2011), Electric Proc. of ISAP 2011*, Oct. 2011.
2. Migliore, M. D., "On the role of the number of degrees of freedom of the field in MIMO channels," *IEEE Transactions on Antennas and Propagation*, Vol. 54, No. 2, 620–628, Feb. 2006.
3. Quist, B. T. and M. A. Jensen, "Optimal antenna radiation characteristics for diversity and MIMO systems," *IEEE Transactions on Antennas and Propagation*, Vol. 57, No. 11, 3474–3481, Nov. 2009.
4. Recioui, A. and H. Bentarzi, "Capacity optimization of MIMO wireless communication systems using a hybrid genetic-taguchi algorithm," *Wireless Personal Communications*, Vol. 71, No. 2, 1003–1019, Springer, 2013.
5. Olgun, U., C. A. Tunc, D. Aktas, V. B. Erturk, and A. Altintas, "Optimization of linear wire antenna arrays to increase MIMO capacity using swarm intelligence," *The Second European Conference on Antennas and Propagation, 2007. EuCAP 2007*, No. 1–6, Nov. 11–16, 2007.
6. Reichardt, L., J. Pontes, W. Wiesbeck, and T. Zwick, "Virtual drives in vehicular communication," *IEEE Vehicular Technology Magazine*, Vol. 6, 54–62, May 2011.
7. Reichardt, L., J. Maurer, T. Fugen, and T. Zwick, "Virtual drive: A complete V2X communication and radar system simulator for optimization of multiple antenna systems," *Proceedings of the IEEE*, Vol. 99, No. 7, 1295, 1310, Jul. 2011.
8. Pontes, J., L. Reichardt, and T. Zwick, "Investigation on antenna systems for Car-to-Car communication," *IEEE Journal on Selected Areas in Communications*, Vol. 29, 7–14, Feb. 2011.
9. Pontes, J., *Optimized Analysis and Design of Multiple Element Antennas for Urban Communication*, Ph.D thesis, Karlsruhe Institute of Technology, 2010.
10. Reichardt, L., T. Mahler, Y. L. Sit, and T. Zwick, "Using a synthesis methodology for the design of automotive antenna systems," *Proceedings of the European Conference on Antennas and Propagation, EuCAP 2013*, Gothenburg, Sweden, Apr. 2013.
11. Reichardt, L., T. Mahler, T. Schipper, and T. Zwick, "Influence of single and multiple antenna placements on the capacity of C2C communication systems," *Proceedings of the European Microwave Conference 2013, EuMC 2013*, Nuernberg, Germany, Oct. 2013.
12. Sit, Y. L., L. Reichardt, R. Liu, H. Liu, and T. Zwick, "Maximum capacity antenna design for an indoor MIMO-UWB communication system," *In Proceedings of the 10th International Symposium on Antennas, Propagation and EM Theory*, Xian, China, Oct. 2012.
13. Zheng, L. and D. N. C. Tse, "Diversity and multiplexing: A fundamental tradeoff in multiple-antenna channels," *IEEE Transactions on Information Theory*, Vol. 49, 1073–1096, May 2003.

14. Gesbert, D., M. Shafi, D. Shiu, P. J. Smith, and A. Naguib, "From theory to practice: An overview of MIMO space-time coded wireless systems," *IEEE Journal on Selected Areas in Communications*, Vol. 21, 281–302, 2003.
15. Wallace, J. W. and M. A. Jensen, "Intrinsic capacity of the MIMO wireless channel," *Proceedings of the 56th IEEE Vehicular Technology Conference*, Vol. 2, 701–705, 2002.
16. Tsoulos, G., *MIMO System Technology for Wireless Communications*, CRC Press, 2006
17. Raleigh, G. G. and J. M. Cioffi, "Spatio-temporal coding for wireless communication," *IEEE Transactions on Communications*, Vol. 46, 357–366, Mar. 1998.
18. Suvikunnas, P., J. Salo, L. Vuokko, J. Kivinen, K. Sulonen, and P. Vainikainen, "Comparison of MIMO antenna configurations: Methods and experimental results," *IEEE Transactions on Vehicular Technology*, Vol. 57, 1021–1031, 2008.
19. Jensen, M. A., and J. W. Wallace, "A review of antennas and propagation for MIMO wireless communications," *IEEE Transactions on Antennas and Propagation*, Vol. 52, 32810–2824, 2004.
20. Klenner, P., S. Vogeler, K.-D. Kammeyer, L. Reichardt, S. Knörzer, J. Maurer, and W. Wiesbeck, "System design for time-variant channels," *OFDM — Concepts for Future Communication Systems*, Vol. 1, 144–150, Springer, 2011.
21. Chizhik, D. "Slowing the time-fluctuating MIMO channel by beam forming," *IEEE Transactions on Wireless Communications*, Vol. 3, 1554–1565, Mar. 2004.
22. Klenner, P., L. Reichardt, K. D. Kammeyer, and T. Zwick, "Spatio-temporal coding for wireless communication," *MIMO-OFDM*, 69–78, Springer, Netherlands, 2009.